Automated morphological classification of galaxies

Elina Lassi
B. Sc. thesis
Degree Programme of Physical Sciences
Faculty of Science
University of Oulu
11.1.2022

Contents

1. Introduction

Ever since large-scale observations of galaxies became possible due to technological development of observational equipment, the number of known galaxies within the universe has gradually increased. This has led to the development of various classification methods to sort galaxies into morphological classes, which has proven to be useful in the effort to try and understand their formation and evolution.

The original 1888 *New General Catalogue of Nebulae and Clusters of Stars* (NGC) by J. Dreyer, with its two *Index Catalogue* supplements from 1895 and 1908, amount to a total of 13 226 catalogued objects. For comparison, Sloan Digital Sky Survey[1] has catalogued more than 50 million galaxies since 2000, whereas the Dark Energy Survey[2] catalogues include more than 200 million galaxies to date. Future surveys, such as Euclid[3] or the Legacy Survey of Space and Time[4], are sure to dwarf their predecessors with the amount of produced survey data. The amount of data collected from modern astronomical surveys has reached such massive proportions that the conventional method of classifying galaxies visually is not practical anymore. Thus, new methods to automate the process and maintain systematic objectivity in the classifications are needed. The creation of new, automated methods requires, however, a lot of human effort put into them before even partial automation can be reached within the classification process.

Citizen science projects such as Space Fluff[5], which focused mainly on identifying low surface brightness objects from the Fornax Deep Survey data (see e.g. Peletier et al. 2020), and Galaxy Zoo[6], which has classified data from for example all Sloan Digital Sky Surveys and has to date ongoing projects, have been established to help with sorting and vetting out different types of objects from large amounts of survey image data. These projects rely entirely on volunteer contributions, albeit Galaxy

[1] `https://www.sdss.org/`
[2] `https://www.darkenergysurvey.org/`
[3] `https://www.cosmos.esa.int/web/euclid/home`
[4] `https://www.lsst.org/about`
[5] `https://www.zooniverse.org/projects/sundial-itn/space-fluff`
[6] `https://www.zooniverse.org/projects/zookeeper/galaxy-zoo/`

Zoo has introduced a convolutional neural network (CNN) trial (Walmsley et al. 2019) alongside the volunteer-driven classification, trained on data received from previous classifications made by users, to present the volunteers with more informative imagery to classify. In addition to being of use directly in research, the classified image data is also useful in the training and development of classification algorithms.

Machine learning as a tool in galaxy classification has been a topic of discussion for decades. Along with the development of computational systems the subject has gradually shifted from being a topic of speculation towards the larger-scale applications that are now reality within the field of astronomy. Computer algorithms which mimic the behaviour of biological neural systems and their ability to recognize relationships within sets of data, also known as neural networks, can, among other things, be trained to recognize, categorize, alter, and combine images. Neural networks can therefore serve as a viable option in the development of new, more efficient galaxy classification tools. The data received from the citizen science projects mentioned earlier is also used to train automated classification algorithms, which can pick up the work from where available human resources can no longer keep up with the growing amount of data.

In chapter 2, I give a general outline of the structural components present in galaxies. In chapter 3 I overview different classification schemes for galaxies, focusing on morphological and non-parametric classification. In chapter 4, I briefly go over the theory of artificial neural network as well as supervised and unsupervised learning methods in the context of galactic astronomy, along with examples of different applications of convolutional neural networks and clustering algorithms.

2. Structural components in galaxies

Galaxies are gravitationally bound systems that consist of stars and dark matter, potentially along with various other components, such as neutral and ionized interstellar gas, molecular clouds and dust. They can be found both in regions of the universe densely populated by galaxies, such as groups and clusters, as well as sparsely populated voids between the more densely populated filaments of the cosmic web. The environment of the galaxy has a strong impact on the evolution and morphology of the galaxy. Galaxies exhibit a variety of observable structural features, based on which division into various classes is possible.

Various classification systems and the bases of each system are discussed in chapter 3 - the focus of this chapter is to give an outline of the morphological features of several main types of galaxies on a very general level.

2.1. Stellar and gaseous halos

A stellar halo within a galaxy is a spherical, diffuse collection of globular clusters and stars thought to have formed from material stripped via tidal interactions from star clusters or satellite galaxies on orbit around the galaxy. Before merging into the halo structure, the stripped material is visible as large, elongated arc-like features around the galaxy. Based on results received from simulations (see e.g. McCarthy et al. 2012), the halo likely consists of two different components, the inner and outer halo which have different origins and physical characteristics. The simulation results suggest that the outer halo forms via accretion of stars, whereas the inner halo forms due to the heating of the protogalactic disk.

The gaseous halo consists mostly of very diffuse gas of varying temperature, along with trace amounts of dust, metals and molecules (H_2, CO). The dust, molecular gas and metals present in the gaseous halo are a result of stellar activity and supernovae in the galaxy. In massive galaxies the gas within the halo can reach extremely high temperatures, which can be detected via x-ray radiation. The gas of the halo has several possible origins (see e.g. Putman et al. 2012): a galaxy can accrete

new gas into its halo from the intergalactic medium (IGM) along cosmic filaments or capture gas from its satellite galaxies. Gas can also be recycled between the disk and the halo within a galaxy via so-called galactic fountains, a term first coined by Shapiro and Field (1976). Expansion of cavity bubbles fueled by stellar winds or supernova activity within star clusters can blow out disk material into the halo and thus cause the mixing of metal-rich disk gas and metal-poor halo gas (Mac Low and McCray 1988).

2.2. Disks

A galactic disk is a highly flattened rotating component containing most of the stars in the galaxy, accompanied potentially by gas and dust, and described by its exponentially falling surface brightness profile. The appearance of a disk varies from a featureless, smooth one to that of a spiral galaxy, with its characteristic spiral arm structure. Galaxies feature both thin and thick disks. Thick disks contain mostly old, metal-poor stars, and their origins is a subject of debate. Several formation methods have been proposed: these include, for example the suggestion by Villalobos and Helmi (2008) that the formation of a thick disk is possible after the galaxy is heated during a major merger event, whereas Loebman et al. (2011) present a model where the thick disk forms through radial migration of stars. The stellar populations in thin disks are far younger and more metal-rich than those in thick disks, due to being the result of star formation caused by gas accretion later in the galaxy's formation history (see e.g. Yoachim and Dalcanton 2006). Both the scale height and length of the thin disk are also lower than those of the thick disk. The thin disk is, thus, embedded inside the thick galactic disk.

The disk can accrete material from the surrounding interstellar material, thus gaining new material for forming stars. Active star formation eventually incites supernova activity in the disk, followed by transfer of disk material into the surrounding gas halo as described in chapter 2.1.

2.3. Spiral arms

Spiral arms are dense structural features that appear within the galactic thin disk, manifesting as several curved bright strands of stars and interstellar matter. The appearance of spiral arms largely varies from well-defined, long and luminous arms to patchy, irregular and relatively less luminous ones.

Density waves which induce star formation by moving through the gaseous disk structure were proposed as the explanation for spiral arms

by Lin et al. (1969) as an attempt to explain the persistence of a spiral pattern in a galaxy. The density waves that make up the spiral arms move through the thin disk far slower than the average ISM and stars within the disk, compressing disk gas and causing subsequent star formation visible as bright blue regions in the arms.

Seigar and James (1998) have speculated that the determining factor for the arm type of a spiral galaxy is the cold gas content of the galaxy. This is because the amount of cold gas within a galaxy controls the amount of star formation, thus affecting the distribution of young, bright stars. Similarly, a relationship between the mass of the central supermassive black hole of a galaxy and the pitch angle of the spiral arms has been proposed by Seigar, Kennefick, et al. (2008): the larger the mass of the black hole, the smaller the pitch angle. The pitch angle refers to how tightly the arms are woven around the center of the galaxy - a large pitch angle corresponds to wide open arms far apart from each other, whereas a small one refers to spiral arms tightly wound together and around the galactic center.

2.4. Central bulges

A bulge is a concentration of mass within the central region of the galaxy. It is less flattened than the disk of the galaxy, and visible as a region of higher brightness that departs from the disk's exponential surface brightness profile. According to Athanassoula (2005), bulges can be roughly divided into classical bulges, boxy-/peanut-shaped bulges and disk-like bulges. The latter two are two distinct sub-types of pseudobulges, a term which sets them apart from classical bulges. Pseudobulges can be characterized as bulges with active star formation, young stars and rotating kinematics, whereas classical bulges are akin to elliptical galaxies in their features, such as random-motion dominated kinematics and a smooth distribution of old stars. Different types of bulges can co-exist in the same galaxy: composite bulges with both a classical and a pseudobulge component have been identified and studied by for example Erwin et al. (2015).

Different formation methods have been proposed for classical bulges. For example, Aguerri et al. (2001) have suggested that classical bulges have formed in the early universe via accretion of dense satellites which caused the growth of the bulge, whereas Noguchi (1999) has proposed that the bulge has merged from the clumps of the disk material caused by gravitational instabilities in the early evolution phases of the galactic disk.

Boxy/peanut bulges are thought to have formed from a vertical insta-

bility in a galactic bar. The characteristic shape of the bulge is a result of bar material detaching from the equatorial plane in a galaxy. Athanassoula et al. (2015) have shown that this type of a bulge and a so-called barlens, first unambiguously identified by Laurikainen et al. (2011), are in fact the same thing viewed from different angles. Disk-like bulges, on the other hand, are formed via infall of mainly gas into the central regions of a galaxy or via gas redistribution within the disk. The gas subsequently forms an inner disk, which makes up the disky pseudobulge.

Within the bulge of a larger galaxy, the abundance of gas may trigger generous amounts of star formation, resulting in what is called a nuclear star cluster (NSC) at the innermost regions of the galaxy. NSCs are common: within the late-type galaxies, it has been estimated (Böker 2009) that at least half of early-type spirals feature a NSC, compared to 75% of late-type spirals. Nuclear star clusters can also form in smaller galaxies via the migration of globular star clusters towards the central region of the galaxy (Tremaine et al. 1975).

What has and hasn't been considered a bulge, especially in older studies, varies greatly depending on the author's interpretation: what would nowadays be explicitly referred to as a bulge has historically been grouped under varied terminology, ranging from "unresolved nuclear regions" to "amorphous center regions" and "peculiar nuclei". A systematic approach towards the classification and study of bulge components is a relatively new prospect.

2.5. Bars, lenses and rings

A galactic bar is an elongated structure in the central region of some disk galaxies. Formation of a bar in a galaxy can be either incited by internal gravitational instabilities in the thin disk or by disturbances caused by interactions with other galaxies, leading to disturbed stellar orbits that begin to deviate from circular orbits and eventually form the galactic bar. Along with a larger bar, some galaxies also contain a nuclear bar, which is a smaller bar nested within the larger bar component (see e.g. Friedli and Martinet 1993).

Lenses are somewhat spherical components present in some galaxies, with shallow inner brightness gradients limited by a sharp outer edge and located between the bulge and the disk, coexisting with a galactic bar.

Rings are features of varying size and structural integrity within the galaxy. A partially defined or open ring is called a pseudoring, as opposed to a classical ring with a closed structure. They range from outer rings, which are, as the name suggests, ring-like collections of stars in the outer regions of the galaxy, to inner and nuclear rings, which in turn are rings

in the inner and nuclear regions.

3. Galactic classification schemes

Various classes of galaxies can be defined in order to establish a foundation from which further research can be conducted. For such classification scheme to be useful in practice, it should without ambiguity distinguish between the different defined types of galaxies and have a physically motivated basis.

Every classification system is always a product of its time, built upon what observational data and constrained by what technical means to extract and analyze it were available. Especially the older schemes are systematically developed based on observations of giant, luminous and fairly well resolved galaxies of the nearby universe, in the absence of observational instruments that could peer deeper into the less luminous and distant parts of the universe. Attempts to fit low surface brightness irregular galaxies - potentially at higher redshifts - into older schemes often fall short, as the schemes were not made with such galaxies in mind and thus cannot properly accommodate them. The perceived morphology is also affected by the wavelength the galaxy is imaged on. The prominence of a morphological feature when observed in a certain wavelength depends on the stellar population and the gas content within the feature.

3.1. Morphological classification

3.1.1. Hubble classification scheme

An example of a classification system is the Hubble system (Hubble 1926), later followed by the Hubble 'tuning fork' scheme (Hubble 1936; see figure 3.1). The system can be considered to be the first and to date perhaps most widely used of all classification schemes despite, as stated by its creator, its "descriptive and entirely independent of any theory" nature. It should be noted that the original scheme did not speak of different types of galaxies as such, but rather referred to them as 'extra-galactic nebulae' - the nomenclature has since changed to simply 'galaxies'. The scheme divides galaxies into classes of ellipticals of varying ellipticities (E0 - E7), irregular (Ir) and spiral galaxies. Of these, spiral galaxies are sectioned into ordinary (non-barred, S) and barred

spiral galaxies (SB), and further into early (a), intermediate (b) and late (c) types within both sub-classes.

Elliptical galaxies are defined by Hubble (1926) as objects in which the only notable structure is the gradually diminishing luminosity from the central areas towards the peripheral regions of the galaxy. They are divided into subgroups En, where n = 0, 1, ... , 7, depending on the apparent axial ratio $\frac{b}{a}$ and thus the perceived ellipticity of the galaxy. The value of n is determined by the formula

$$n = 10(1 - \frac{b}{a}),$$

in which n increases along with the ellipticity of the galaxy, E7 being thus the most and E0 the least elliptical.

For spiral galaxies of both the unbarred and barred variety, Hubble (1926) considers the classification of different galaxies in the group on the grounds of the relative size of the "unresolved nuclear region", the extent to which the arms are unwound, and the degree of resolution in the galactic arms. Spiral galaxies with well resolved, tightly wound together arms and large nuclear regions are denoted as Sa, whereas galaxies with flocculent, spread out arms and small nuclei are labeled as members of the Sc group.

Irregulars are defined by Hubble as galaxies which lack both a dominant nucleus as well as rotational symmetry. Hubble proposed two different classes of irregulars, denoted Ir I and Ir II. Neither of these types have structural symmetry, but they differ from each by their other characteristic features. Ir I galaxies are described as a "homogenous group" that shares features with the Magellanic Clouds, with stellar content resembling that of late-type spirals. They're placed in the scheme as the last stage of galaxies following the extreme late-type spirals, albeit this is not reflected in the visualization of the tuning fork diagram (see figure 3.1). Ir II galaxies are described as a heterogeneous class of highly peculiar objects. Hubble makes a note that this classification is not truly physically or morphologically justified, and is rather used as a dump for the leftover galaxies not fit for any of the other defined classes.

The original classification scheme by Hubble (1926) does not include lenticular galaxies. The group was added into the scheme later: Hubble (1936) defines lenticular galaxies as intermediate objects between E7- and Sa-class objects. The new class is not given much attention: S0 is referred to as a hypothetical class merely established to 'solve' the observed discrepancy between the transition from E7 ellipticals to Sa spirals.

A major problem in establishing the Hubble system, also acknowledged by Hubble (1936), was the inadequate availability of detailed enough

photographic data of faint galaxies and the more subdued features of brighter galaxies to be able to account for the intricate details within different types of galaxies. The choice of the various sub-classes is a compromise set by technical limitations, despite the already then suspected variability of the more intricate features in galaxies. Hubble (1936, p. 37) states that "*[i]nconspicuous features, although they might be highly significant, would restrict the classification to a small number of nebulae which might not be a fair sample*".

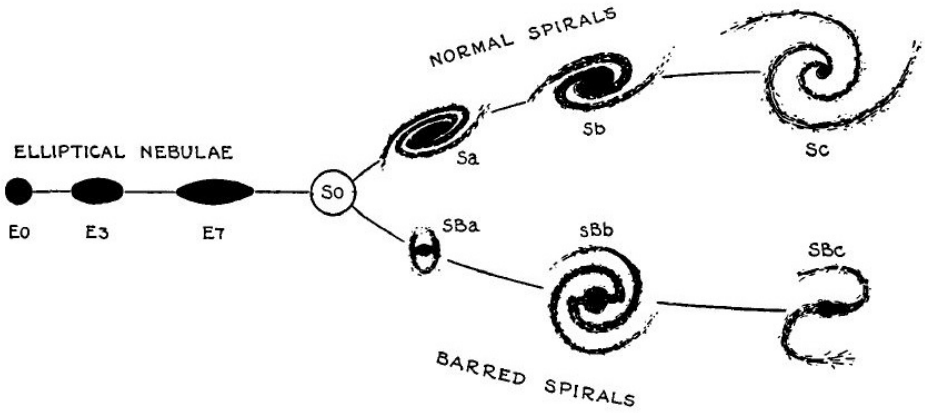

Figure 3.1: The original Hubble sequence. *Reprinted by permission from Springer Nature Customer Service Centre GmbH: Springer Nature, Nature, The Realm of the Nebulae by E. Hubble. Springer Nature 1936.*

The Hubble system has later been found to be lacking also in terms of how ellipticals are classified compared to types towards the late end. For example, Kormendy and Bender (1996) point out that the classification for ellipticals from type E0 up to type E6 is more due to the apparent inclination of the galaxy than any physically interpretable reason. The suggested improvement to better account for the fundamental properties of the elliptical galaxies is to base the sequence of E galaxies on the shape of their isophotes, resulting in sub-types of ellipticals ranging from boxy to elliptical to disky types. The true shapes of ellipticals feature various levels of triaxiality, which can be described by for example the triaxiality index T (see e.g. Franx et al. 1991) which sorts ellipticals into prolate, triaxial and oblate based on their axial ratio.

3.1.2. De Vaucouleurs' classification scheme

Further improved and altered versions, of which some are based on the original Hubble classification, have later been developed. The sought

after recognition of smaller details within galaxies came about in the revised Hubble scheme proposed by de Vaucouleurs (1959), also known as the de Vaucouleurs revised Hubble-Sandage (VRHS) system. The revised system takes into account the lenticular and ring-like features in the disk of the galaxies, along with the existence of an intermediate type of spiral galaxy, denoted SAB, and lenticular galaxies of both the ordinary (non-barred) and barred variety, denoted SA0 and SB0, respectively. As with spirals, an intermediate type is also recognized, denoted SAB0. SA0's and SB0's are situated at the crossroads of elliptical and spiral galaxies, serving as a transitional type between the two. Some of the galaxies classified earlier as for example early SBa's were subsequently re-classified as SB0's.

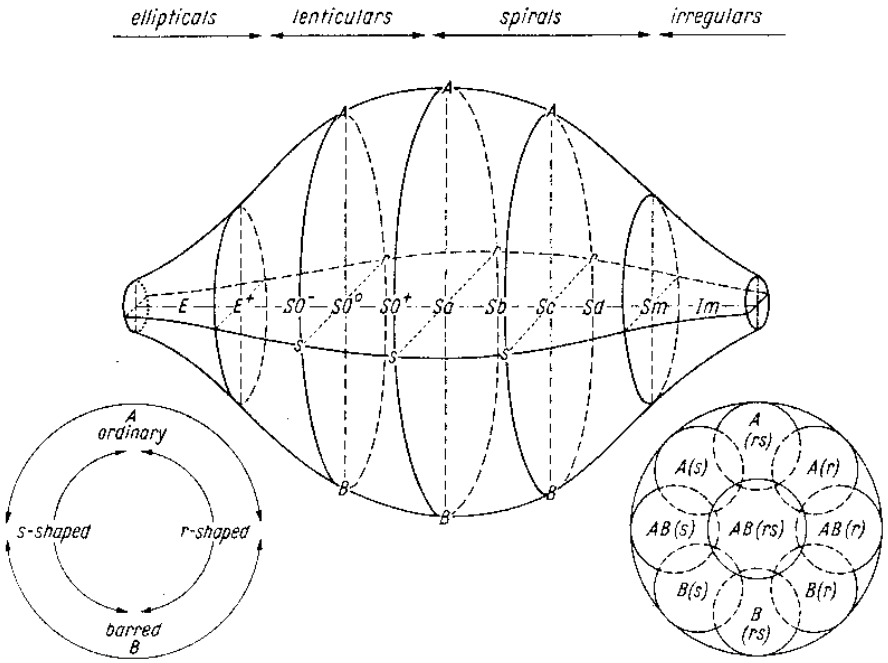

Figure 3.2: Visualization of the de Vaucouleurs classification scheme.
Reprinted by permission from Springer Nature Customer Service Centre GmbH: Springer Nature, Classification and Morphology of External Galaxies by G. De Vaucouleurs. Springer-Verlag OHG, Berlin 1959.

The scheme also recognizes various stages within the main types of early-type galaxies. For example, lenticular galaxies are divided into early ($S0^-$), intermediate ($S0^o$) and late ($S0^+$) sub-classes, which allows for more finesse in the classification of lenticular galaxies by establishing classes akin to the transitional classes of spirals (ab, bc, cd). Some of the original Hubble notations, such as simply E7 or S0 still exist in the system, but are only ever used to denote a galaxy which is viewed

completely edge-on. These systems are marked with the notation (sp), short for 'spindle'.

Within the already established types, the late-end sub-typing of spirals was extended to cover types d and m, which are set in the scheme after the initially established sub-types a-c, before the irregular (Im) galaxies. Spiral galaxies, along with the newly established type of lenticular galaxies, are sectioned into galaxies of ringed (r) and galaxies of spiral (s) variety, as well as galaxies of the intermediate type (rs). The notation m refers to 'magellanic' features resembling those of the Magellanic clouds - for example, the Large Magellanic Cloud (see figure 3.3) is SB*(s)m* in the de Vaucouleurs system. The additional features in the system are represented by a third axis, making the classification scheme three-dimensional as can be seen from figure 3.2.

Additionally, dwarf ellipticals (dE), which went by the name 'Sculptor type' for a time, were recognized as a separate type of galaxy following the discovery of the Sculptor and Fornax systems by Shapley (1938).

Figure 3.3: The Large Magellanic Cloud is considered to be of the type SB*(s)m* in the de Vaucouleurs system and Ir I in the Hubble system.

van den Bergh (1998) criticizes de Vaucouleurs' scheme for the simultaneous drop in luminosity and the gradual transition to blue being both attributed to a single classification parameter when moving along to the right in the classification sequence Sc-Sd-Sm.

3.1.3. Morgan's classification scheme

Similar to the de Vaucouleurs classification system explored in chapter 3.1.2, the Morgan (1958) system for classifying galaxies is a modified version of the Hubble system. The scheme is based on the assumed

correlation between the central concentration of light and the average stellar population within the galaxy estimated from its composite spectrum. The Morgan system was developed due to an observed lack of real correlation between the spectral types and the Hubble morphological class in case of some classes, a problem present mainly in different stages of spirals of both the ordinary (S) and the barred (SB) variety. The aim of Morgan's classification is to accurately portray the stellar population of the galaxy on a general level within each type of galaxy. The assigned type of a galaxy is a combination of three parameters used in the classification scheme to describe the central concentration of the light, the 'form family' and the approximate tilt of a flattened system.

Within the fundamental parameter, galaxies are grouped into four main categories of *a*, *f*, *g* and *k* based on the central concentration of light within the galaxy, taking also into account the intermediate types between two main ones, such as *af* or *gk*. Of these, objects of the *a* type have the weakest and objects of the *k* type the strongest central concentration of light, the rest being intermediates between the two extreme ends. In type *a* galaxies the light is dominated by B-, A- and F-type stars, whereas the light of *k*-type galaxies is mainly dominated by large, old K-type stars.

The first secondary parameter for the 'form' of the galaxy overlaps somewhat with the Hubble classification, recognizing elliptical (E), irregular (I) and both barred (B) and ordinary (S) spiral galaxies. Additionally, systems with low surface brightness (L) as well as systems with a bright nucleus and subdued background (N), systems with a star-like appearance with large redshifts in their spectra, also called quasi-stellar objects (Q), and systems with a large, diffuse envelope showing rotational symmetry, yet lacking a spiral or an elliptical structure (D) are recognized. The other secondary parameter describes the approximate level of tilt of a galaxy as seen by the observer. This 'inclination class' parameter is, however, not used for irregulars, low surface brightness systems or certain barred spirals.

Later, the N type was further divided by Morgan (1971) into subcategories N-, N and N+ in an effort to establish an internally consistent way to classify N-type galaxies. N- includes galaxies with relatively less pronounced nuclei compared to the other N-type galaxies, whereas N+ galaxies feature an extremely bright nucleus and a markedly subdued background, possibly with for example spiral arms or jets. N serves as an intermediate type between the two.

Criticism towards the Morgan system stems from the seemingly arbitrary criteria for D-type galaxies within the form family parameter. The criteria for a galaxy to be considered as a D-type overlaps, according to

for example van den Bergh (1998), with that of S0's and E's in terms of including galaxies with S0-like disks and tidally stretched halos, thus rendering the D-type somewhat useless as an effective classification tool.

3.1.4. Van den Bergh's parallel classification scheme

A classification system by van den Bergh (1976) redefines the sequence of classically late-type systems within Hubble (1936) based on their gas abundance and bulge-to-disk ratios. The reason behind the reassembly of the classical scheme is the perceived hypothetical nature of the transition from E through S0 to the Sa-Sb-Sc-sequence.

The redefined sequence parallels the S0 galaxy sub-types with the traditional sequence of S galaxies. Additionally, an intermediate type of 'anemic galaxies' is introduced as its own sequence. Of these, the S sequence features the gas-rich systems, whereas the S0 sequence represents the gas-devoid systems. van den Bergh (1976) points out that since both the S0 and S types have very similar axial ratios (i.e. both are intrinsically very flattened; Sandage, Freeman, et al. 1970) and mainly differ in the abundance of gas in their structure, the existence of a gas-poor 'anemic' intermediate type is possible. These three sequences could, thus, be paralleled with each other. The resulting trident-shaped scheme is presented in figure 3.4.

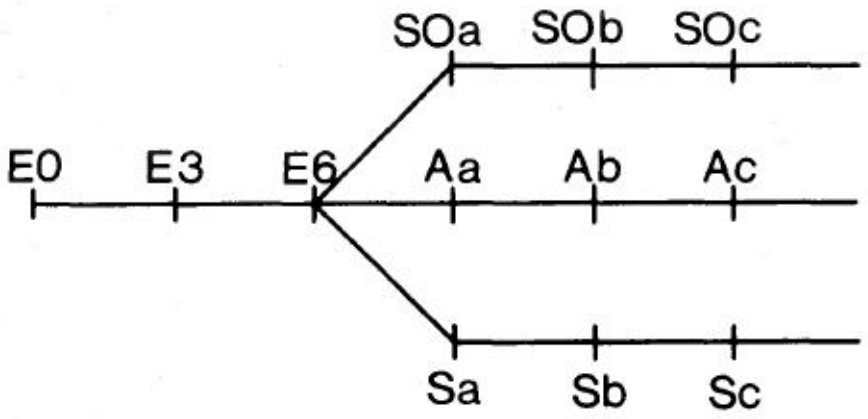

Figure 3.4: The parallel classification system as proposed by van den Bergh (1976).

Observational evidence to support the scheme came about decades after it was initially published, as for example true S0c lenticulars were

documented by Laurikainen et al. (2011). The idea of a paralleled sequence is seconded also by for example Kormendy and Bender (2012), who in addition propose extending the S0 branch by relating the late end to spheroidal (Sph) galaxies, somewhat analogous to the Im galaxies in the S branch. This, according to the authors, creates a continuous sequence from early-type S0s with large bulges all the way to Sphs with no bulge at all.

On the other hand, it has been questioned whether paralleling the sequences of the trident is justified. Graham (2019) argues that the true 'overlap' between the three branches of the trident is in fact minimal compared to how the scheme was initially presented. The average bulge-to-disk ratio of early-type disk galaxies is far higher than that of spiral galaxies, and the amount of for example early-type disk galaxies with B/D values resembling those of extremely late-type spirals with barely any bulge is not significant enough to justify the shape of the trident. Graham (2019) suggests that the overlap of the paralleled sequences in the classification trident is, at best, partial, and that the parallel prongs of the trident should be established based on the strength of the galactic bar.

3.1.5. Elmegreens' classification scheme for spiral arms

Within spiral galaxies, the variance of the spiral arm structure has been documented on a larger scale since Reynolds (1925), who remarked that the arms of the reviewed spiral galaxies exhibit patterns from well-defined tightly wound together arms to patchy ones far apart from each other. A classification system by Elmegreen and Elmegreen (1982) divides spiral galaxies into 12 different categories based on the length, continuity and symmetry of the spiral arms. The types range from *1* to *12*, where galaxies of type *1* have a 'chaotic appearance' with no symmetry and ragged arms with varying pitch angles, whereas galaxies of type *12*, also called "grand design galaxies" by the authors, feature two sharp-featured, long, symmetric arms that dominate the structure of the galaxy.

The classification scheme was devised based on a study by Elmegreen and Elmegreen (1982) of galaxies isolated in the field, those in binary systems and those in groups, accompanied by Elmegreen, Elmegreen, and Dressler (1982) in which galaxies in cluster environments were similarly classified. It was found that the designated arm class correlates fairly well with the presence of a bar, as well as the presence of a companion galaxy. The strongly defined so-called "grand design" arms are more common among galaxies with either a bar or a companion galaxy, and fragmented, unevenly spaced arms occur more commonly in isolated, non-barred (corresponding with the main Hubble type SA) galaxies.

Later, the arm classes *10* and *11* were abolished (Elmegreen and Elmegreen 1987) and the galaxies previously classified as such were reclassified. The galaxies of class *10* were barred galaxies and those of class *11* galaxies with one or several close companions.

3.1.6. Comprehensive de Vaucouleurs revised Hubble-Sandage classification scheme

As a modernized variant of the VRHS scheme discussed in chapter 3.1.2, the comprehensive de Vaucouleurs revised Hubble-Sandage classification scheme (CVRHS, discussed in detail by e.g. Buta, Sheth, et al. 2015; Buta 2019) seeks to define and classify previously somewhat undocumented features which affect galaxy structure and evolution and also to set a standard for possible future studies applying automated classification to large samples of galaxies. CVRHS recognizes several different characteristic features of galaxies: the stage, family, possible outer and inner variety as well as the nuclear variety of the galaxy. Along with these, cataclysmic rings resulting from major interaction events and edge-on galaxy collisions are taken into account in the scheme.

The stage of a galaxy refers to the development of the structure, distribution of star formation, importance of the bulge component relative to the rest of the galaxy, integrated colour, average surface brightness as well as the HI mass-to-blue luminosity ratio. The family refers to the apparent strength of a bar or some other structure, such as an X-shaped (e.g. SAB_x) or an oval (S$\underline{A}$B) inner structure.

For the inner and outer variety, the inner variety refers to the absence or existence of an inner ring and the outer, in turn, the presence of a possible outer ring or a pattern resembling a ring. Additionally, special-case scenarios for both inner as well as the outer varieties are recognized. These include for example the presence of several outer or inner rings or pseudorings (e.g. rr, RR, rs, R'R'), a barlens (bl, Laurikainen et al. 2011) which is a ring-like part of a bar, as well as the presence of a lens with a subdued spiral-like pattern (ls).

The nuclear variety, as suggested by the name, recognizes various features, such as rings (e.g. nr, refer to Comerón et al. 2010), bars (e.g. nb), ring-lenses (nrl) etc. commonly found at the centers of barred galaxies and occasionally also in non-barred ones. The nuclear variety features can coexist in a combined form with certain inner variety features: for example the existence of both an inner ring as well as a smaller nuclear ring (r, nr) is recognized in the scheme.

Cataclysmic rings are shaped by catastrophic interaction events between galaxies. The types of cataclysmic rings recognized in the scheme include for example peculiar rings (RG) thought to originate from special

galactic collisions, and accretion rings ((R)E) formed from a companion galaxy being disrupted into an orbit around an elliptical galaxy. The latter is also known as a 'Hoag's object' - Schweizer et al. (1987) were the first to suggest that the structure is a remainder left behind by a major accretion event from 2 to 3 Gyr ago.

A comprehensive list with descriptions and notations for all the recognized sub-types of the aforementioned varieties is included in Buta, Sheth, et al. (2015).

3.1.7. Morphological classification of dwarf galaxies

The schemes mentioned so far are mostly built around observations of large and relatively bright galaxies. Galaxies with $M_V \geq -18$ are referred to as dwarf galaxies - this limit for the magnitude is used by for example Grebel et al. (2003), but can vary from author to author.

Sandage and Binggeli (1984) propose a classification system for dwarf galaxies in which the luminosity and the Hubble type of a galaxy form the basis for the classification. The system recognizes dwarf ellipticals (dE), dwarf lenticulars (dS0) and blue compact dwarfs (BCD), and attempts to relate them with the classical Hubble types. A visualization of the scheme is presented in figure 3.5.

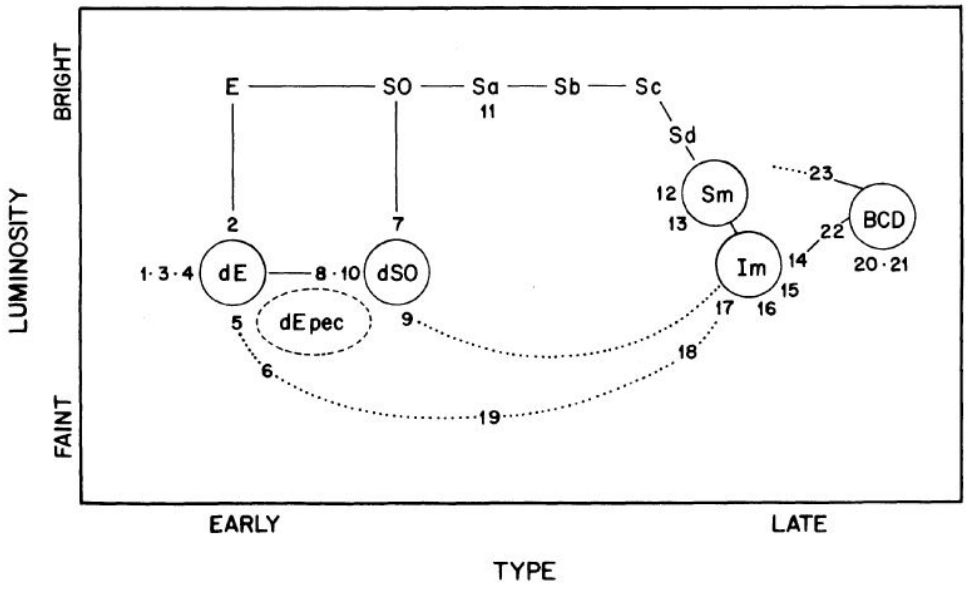

Figure 3.5: Classification system for dwarf galaxies as proposed by Sandage and Binggeli (1984). The dotted lines mark a possible connection between the indicated types.

Of the early-type variety, dEs are defined by Sandage and Binggeli (1984) as galaxies with low surface brightness and a smooth, spherical appearance, and dS0s as galaxies which, on par with S0s, consist of a disk and a bulge component, but differ from their larger counterpart by their low surface brightness.

Within the late-type dwarfs, BCDs are described as galaxies with a very centrally concentrated star-forming region, appearing as one or several bright dense areas within the galaxy's innermost parts, contrasting an otherwise quiescent outer areas. Sm and Im, referred to together as dIrr galaxies, are defined as the extreme low luminosity late end of the disk galaxies in the Hubble sequence. Star formation in dIrr galaxies happens actively across the whole galaxy.

3.1.8. Morphological classification of galaxies at higher redshifts

As was the case with the morphology and classification of dwarf galaxies (chapter 3.1.7), the prevalent galaxy classification schemes are also ill-fitted for classifying galaxies further away in the universe. van den Bergh (2002), for example, asserts that the classical Hubble scheme is suitable only for classifying galaxies with a redshift $z \leq 0,5$. The amount of merger activity increases with the look-back time, as does the relative amount of highly irregular and clumpy galaxies. The star-formation of galaxies at high z is for the most part driven by mergers, as opposed to the star-formation mostly taking place in disks at low z. Albeit no comprehensive morphological classification scheme for galaxies at higher redshifts exists, attempts to divide the observed galaxies based on their appearance have been made.

Elmegreen, Elmegreen, Rubin, et al. (2005) have identified various morphological classes for the galaxies in the Hubble Ultra Deep Field (UDF). The different types are divided by the authors into chain, double-clump, tadpole and clump-cluster galaxies. These kinds of galaxies have been recognized individually in earlier works by for example van den Bergh (2002), who mentions both comma- and tadpole-like galaxies (distinction between the two made based on their 'tail' length) as well as chain-like galaxies. All of the galaxies identified here that deviate from the Hubble 'norm' share several common features, such as the presence of very active star formation, as well as the lack of both a bulge and an exponential disk light profile. Many of the galaxies are also low in luminosity and highly asymmetrical in structure.

Tadpole galaxies have a dominant single clump which is linked to a less resolved, tail-like component. Double-clump galaxies are dominated by two clumps, and chain galaxies by several clumps that together make up a chain-like structure. Clump-clusters, in turn, appear as an irregu-

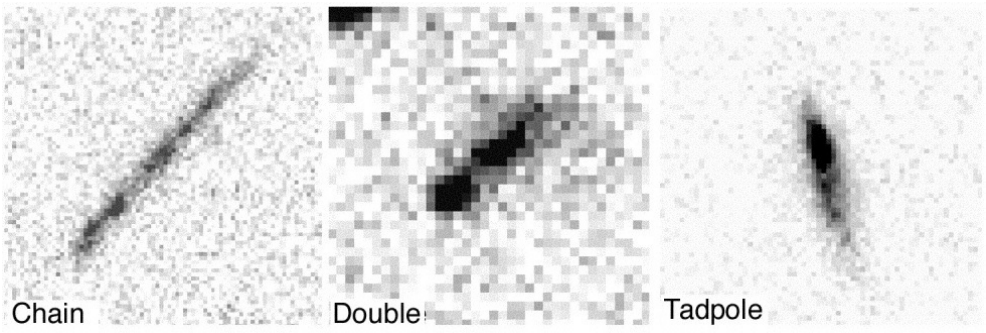

Figure 3.6: Images of chain, double-clump and tadpole galaxies as identified by Elmegreen, Elmegreen, and Sheets (2004).

larly shaped collection of clumps. Elmegreen, Elmegreen, Rubin, et al. (2005) note that for example tadpoles, double-clumps and clump-cluster galaxies might all be different-sized versions of each other.

The evaluated survey data also includes galaxies classically typed as spirals and ellipticals, though the evaluated population of spirals is described to be very varied, and many of the spirals to have a 'highly disturbed' appearance. The relative amount of observed barred spirals also decreases with increasing redshift (noted also by van den Bergh 2002), albeit this could partially be due to the difficulty of spotting a bar structure from a highly irregular galaxy as opposed to one with a more ordered appearance, such as a classical "grand design" spiral.

3.2. Non-parametric classification

The schemes described so far divide galaxies into groups based on either their visual morphology or measured parameters which describe the structure of the galaxy by modelling the distribution of the light within the galaxy. Both morphological and parametric classification systems have been found lacking on several fronts. Morphological classification systems have been criticized (e.g. Conselice et al. 2000; Conselice 2003) for example for their inability to account for the effects of various redshifts on galaxy morphology, and for the entirely descriptive nature of the classification, which does not relate the morphological types to underlying physical processes and is thus not an effective tool in evaluating galaxy evolution. Classical morphological classification systems also do not eliminate subjectivity in the classification process. This is well showcased in for example Naim et al. (1995), where the classifications made by six independent observers on the same sample images were compared with each other. While the observers agreed with each other on a general

level, the results showed "non-negligible scatter".

Parametric classification systems have in turn received criticism (e.g. Lotz et al. 2004) for how single- and multi-component profile fitting, such as the Sérsic index or bulge-to-disk ratio, require the assumption of a symmetric and smooth profile within the evaluated galaxy, as well as an underlying assumption for the form of the light profile, thus rendering the information received model-dependent. The assumption of a symmetric profile shape is not ideal for for example highly irregular or merging galaxies, both of which have noticeably distorted light distribution. This causes the parametric approach to fall short on being able to reliably classify all types of galaxies.

Non-parametric classification attempts to classify galaxies by measuring the light structures within and form a classification system system which relates the results to significant physical features and processes without relying on model parameter fits. The aim is to create a framework for classification which uniquely distinguishes galaxies in different phases of evolution and across a range of redshifts. Out of non-parametric classification systems, the CAS system and the Gini coefficient are discussed here; other non-parametric classification systems such as M_{20} by Lotz et al. (2004) built upon the same principle idea exist.

3.2.1. CAS

The 'CAS' system compiled by Conselice (2003) models the galaxy's stellar light distribution. This is done via three structural indices, which measure the concentration (C), asymmetry (A) and clumpiness (S) of the light within the galaxy, forming the so-called CAS volume within which all classified galaxies are meant to fall.

The concentration index C measures the concentration of light at the center of the galaxy compared to its outer parts. This is measured by taking the ratio of light at two determined radii, for which the central location used is often the same as the one used for measuring asymmetry. A high value of concentration indicates a greater amount of light concentrated at the galactic center. The index scales with the bulge-to-total light ratios, as well as the scale of the galaxy.

The asymmetry index A is used to describe how much of the light of the galaxy is within its asymmetric components - a high value indicates the presence of a relatively large fraction of light within asymmetrical structures. Asymmetry is determined by subtracting an image of the galaxy rotated 180° along its central axis from the original image. Conselice (2003) asserts that the asymmetry index serves as a simple indicator of galactic mergers and galaxy interactions underway.

The smoothness index S describes how large a portion of the galaxy's

light is in clumpy portions of the galaxy. A high value of S indicates a greater amount of light situated in the clumpy regions, and tends to correlate with ongoing star formation within the galaxy. Smoothness is determined by generating a secondary image from the original image by blurring it and then subtracting the secondary image from the original one. What is left as a normalized residual map contains only the high spatial frequency structures of the galaxy. Conselice (2003) argues that star formation is a defining aspect in both the placement of galaxies in the classical Hubble-based morphological classification sequences, as well as when evaluating the evolution of galaxies. In for example the Hubble morphological sequence, early-type galaxies exhibiting barely any star formation, whereas late-type galaxies are morphologically dominated by it. The passive evolution of the galaxy's star population directly affects the morphology of the galaxy, thus serving as a potential aspect to be considered when studying galactic evolution.

Lotz et al. (2004) point out that when measuring the concentration of light at different distances from the center of the galaxy, the use of circular apertures is forced, as is defining a center for the galaxy. This is not ideal for for example irregular galaxies due to their often highly garbled shape, for which it can be almost impossible to unambiguously define a center. In the case of asymmetry as a descriptor for merger galaxies it is noted that, despite the sensitivity of the index for signature features of mergers, not all merger remnants are highly asymmetric, and neither are all of the asymmetric galaxies mergers.

3.2.2. Gini coefficient

The Gini coefficient (G) for galaxy classification (e.g. Abraham et al. 2003; Lotz et al. 2004) is an adapted form of the perhaps more universally known Gini coefficient (also Gini index or Gini ratio), which is used to measure the degree of inequality within a distribution, in economics often the wealth distribution within a society. When evaluating galaxies, G describes the relative distribution of flux within the pixels associated with a galaxy. For a discrete population, such as the pixels in a galaxy, the coefficient is defined as the mean of the absolute difference between all X_i, following

$$G = \frac{1}{2\overline{x}n(n-1)} \sum_{i=1}^{n} \sum_{j=1}^{n} |X_i - X_j|,$$

in which n is the number of pixels in a galaxy and $\overline{x}$ is the mean over all (pixel flux) values X_i. In the case of extreme concentration of flux into one point source, $G = 1$, and a completely equal distribution of flux among the pixels, $G = 0$.

For the majority of local galaxies, G correlates (Abraham et al. 2003) with the concentration parameter C (see chapter 3.2.1), which is due to very centrally concentrated galaxies having most of their light within a small number of pixels. The two indices differ, however, in how they interpret the large-scale distribution of light within the galaxy structure. For example, a galaxy with light concentrated in a non-central part of the galaxy would have a high G, but a low C. This is due to G not making the assumption for the location of the galactic center.

G is affected systematically by the signal-to-noise (S/N) effect on the measurements. Lisker (2008) argues that results from each galaxy could realistically only be compared with those of galaxies with a similar S/N. This is due to how, especially at larger apertures, the systematic effect on results by S/N solely causes the transition within a range of Gini values, instead of it stemming from the actual different surface brightness values of the evaluated galaxies. At smaller apertures, the effect is not as prominent, yet it is still there. As a solution, requiring the difference between the G of different galaxy classes to be larger than the systematic S/N ratio is proposed.

4. Theory and applications of machine learning in galactic astronomy

The morphological classification schemes presented in the previous chapter can be used as a basis for an automated classification system. While the various schemes, especially in the case of older classification systems, have been made with human classifiers in mind, computer algorithms can nowadays also be trained to recognize different types of galaxies from survey image data basing on a classification scheme of choice. Some algorithms can also independently draw conclusions from image data presented to them, creating a galactic classification scheme of their own based on the appearance of galaxies in the data. The topic of neural networks, convolutional neural network -based supervised learning methods and unsupervised clustering methods will be covered on a general level in this chapter, along with recent examples of their applications in galaxy classification.

4.1. Artificial neural networks

Artificial neural networks (ANNs) are computational systems, taking inspiration from the mechanism by which biological nervous systems operate and process information. The basic structure of an ANN comprises of multiple interconnected basic units of the network, neurons, which form layers within the network. These can be divided into the input layer, in-between hidden layers, and the output layer. The number of hidden layers varies - in the case of several hidden layers, the network is a so-called deep neural network. Each neuron, except for the neurons of the input layer, is associated with an activation function. The function determines the node's output when provided with one or several weighted inputs. The weight of the inputs is determined per each neuron-to-neuron connection, and within a network, the output of the previous layer is the input of the next one. The nth layer vector, for example, is defined as

$$\mathrm{x}_n = g(\mathrm{W}_n \mathrm{x}_{n-1} + \mathrm{b}_n),$$

in which g is the activation function, b_n the vector of biases and W_n the matrix that contains the weights for the layer's neurons.

The role of bias in a neural network is to contribute to the output of a neuron by shifting the answer to a desired direction. Bias can be thought of as a constant that is added or subtracted from the output to achieve a better fit for the data within the used model.

The used neuron-to-neuron connections and activation functions within the network determine the network architecture. Common examples are feed-forward networks, radial basis function networks and recurrent neural networks. Of these, feed-forward networks move information in only one direction - from the input towards the output - in the network without any loops within the network structure, whereas recurrent neural networks can move information both forward and backward.

The availability of uniform and large enough data sets as well as the lack of necessary computational power have both constrained the training and use of neural networks as a tool for data processing in astronomy, albeit automated classification methods to evaluate survey data have been hinted at since the 1980's (e.g. Kurtz 1983).

Some of the earliest documented uses include Odewahn et al. (1992), in which stellar and galaxy images were separated from each other with an ANN, and Naim et al. (1995) accompanied by Lahav et al. (1995), where images of galaxies were morphologically classified based on the Revised Hubble T-type system (see e.g. Buta, Mitra, et al. 1994 for a summary of the T-type system) by an ANN trained with a sample classified by several human experts, and the results evaluated on the grounds of how well the ANN matched the human classifiers' classifications. Another noteworthy example from the same time is Weir et al. (1995), where the performance of a supervised neural network is compared to that of a decision tree algorithm in being able to distinguish between stars and galaxies.

4.2. Convolutional neural networks

Convolutional neural networks (CNNs) are fundamentally similar to traditional ANNs. The difference between a CNN and a traditional ANN arises from the possibility to encode image-specific features into the network architecture. The network aims to create a feature map in which the presence of detected features is summarized. In simple terms, the networks takes pixels as an input, identifies and combines the edges detected from the pixels to form shapes, and then uses the formed shapes to detect objects from images.

The CNN structure consist of three main types of layers, which are the convolutional layer, the pooling layer and the fully connected layer. Both

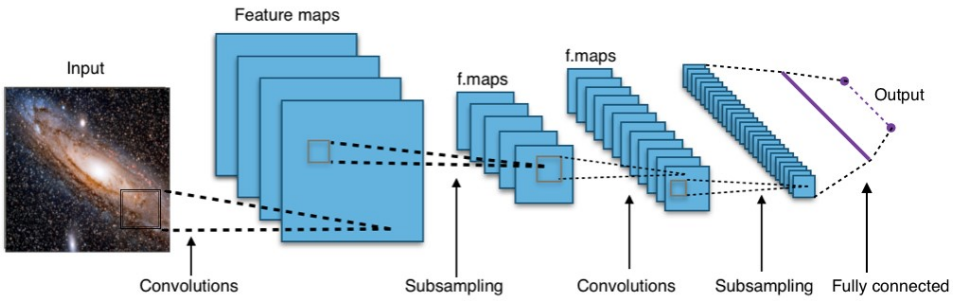

Figure 4.1: Simplified visualization of the convolutional neural network structure. *Distributed under the CC-BY-SA 4.0 license. Original authors of the content used in the adapted version presented here: David Dayag, Aphex34.*

the convolutional and the pooling layers can include multiple instances of the same layer, and the fully connected layer will always follow after these as the final layer of the network. Within the convolutional layer, a filter matrix is applied to a partial area of the processed image, and the network calculates a dot product between the filter values and the pixels of the input. The result gets sent to an output array, and the filter moves on to repeat the procedure within another area of the input image. How much the filter moves is determined by its 'stride', referring to the number of pixels the filter moves vertically and horizontally over the input image. The output of the convolutional layer is passed on to the pooling layer, which subsamples the input given to it in order to reduce the number of trainable parameters.

A CNN learns by a process where a classification is made, checked against the true label in the training data, and the network weights are automatically adjusted to fit the model to better accommodate the training data. The network aims to minimize the value of the loss function that keeps track of the accuracy of the classifications. The learning process is based on training and validation datasets, where - as the names suggest - the training data is used to teach the network and the validation dataset to measure how well the knowledge attained in the training phase can be extrapolated into unseen data. The validation and training losses are tracked separately, and by comparing the two it is possible to estimate whether or not the learning process has been successful.

The learning process of a CNN can stray from the desired result in several different ways: the network can, for example, learn to be too specifically focused on the features on the training data and not be able to extrapolate its knowledge to data outside the training domain, leading to a process called overfitting. One indicator of overfitting can be a growing discrepancy between training and validation loss values during

the training period. The network can also learn to focus on irrelevant features on the data if the training data is not chosen with care to ensure enough variability on the background features around the main object. To avoid overfitting, methods like regularization and dropout can be implemented into the network. Dropout layers randomly set a specific fraction of weights equal to zero, while regularization penalizes larger values of node weights and thus reduces their impact on the training process.

Due to their specific suitability for image recognition and classification, CNNs have been used especially to identify and classify objects from survey image data: examples of such use include morphological classification of galaxies (Dieleman et al. 2015; Aniyan and Thorat 2017), detection of strong gravitational lens candidates and lensing systems (Petrillo et al. 2018; Davies et al. 2019), morphological classification of galaxies into ellipticals and spirals (Cheng et al. 2020), morphological classification into main Hubble types (Cavanagh et al. 2021), separation of low surface brightness galaxies and artefacts from survey images (Tanoglidis, Ćiprijanović, et al. 2020) and further classification of the previously separated low surface brightness galaxies into spirals, dwarf ellipticals and dwarf irregulars (Müller and Schnider 2021).

4.2.1. Binary image-based classification

Most of the CNN applications in galactic astronomy have so far been limited to simple yes-no binary classification tasks, such as whether an object is an artifact or a galaxy, or whether a galaxy is a spiral or an elliptical one. Binary classification tasks are computationally less demanding to execute, and do not require grand amounts of training data to be able to distinguish between two classes, especially if the division is made between two "clear cases", such as point sources and diffuse objects.

As an example, Tanoglidis, Ćiprijanović, et al. (2020) present a CNN-based solution for the overwhelming ratio of false positives while identifying low surface brightness galaxies (LSBGs) from survey images. LSBGs are defined by for example Impey and Bothun (1997) as galaxies in which for the central surface brightness $\mu_0(\mathrm{B}) > 23$ mag arcsec^{-2}.

While identifying LSBG candidates from survey image data, identification algorithms often pick up not only true LSBGs, but also so-called false positive objects which are structurally similar to LSBGs but physically different. False positives that pass the selection criteria of LSBGs include, for example compact, faint objects muddied by the diffuse light from bright stars or giant elliptical galaxies, bright parts of the Galactic Cirrus, which consists of sources that produce background radiation at 100 μ. In addition to these, star-forming dense, bright regions within the

arms of large spiral galaxies and tidal features connected to high surface brightness host galaxies can cause confusion in the algorithm.

The amount of false positives is generally so significant that it vastly outnumbers the amount of real LSBGs in the sample material. This renders the sample contaminated, requiring manual rejection of the artifact objects. For example, in the Dark Energy Survey (DES) after cuts based on colour, the half-light radii in the g-band and the mean surface brightness were performed to exclude artefacts, approximately 8% of the remaining sample were found (Tanoglidis, Drlica-Wagner, et al. 2021) to be real LSBGs.

The network was implemented on the open source machine learning platform TensorFlow[1], making use of its deep learning framework Keras[2]. The structure of the network consist of three 3 x 3 convolutional layers, with the same amount of 2 x 2 pooling layers in between, followed by two fully-connected layers at the end of the network. The training, testing and validation sets used include a sample of labeled LSBGs and artifacts detected from DES (see Tanoglidis, Drlica-Wagner, et al. 2021 for a detailed summary), presented to the network as 64 x 64 RGB pictures.

The performance of the CNN was benchmarked against the results from support vector machine and random forest algorithms, both of which have been widely used in astronomy. The accuracy of the classifications made by the CNN on the same data was found to be significantly better, with a classification accuracy of 92,0%, compared to 81,9% with a support vector machine and 79,7% with a random forest algorithm.

4.2.2. Multi-class image-based classification

Multi-class image-based classification is at its core almost identical to binary classification of the same kind, with the exception of the number of output nodes, the output layer activation function and the loss function used in the training phase. While in binary classification tasks a simple probability between 0 and 1 suffices as an output value, a multi-class classification task requires for the network to be able to produce a result which indicates the probability of the observed object belonging to each defined class. This sets some constraints of what loss and final layer activation functions can be implemented into the network: multi-class CNNs for example usually use the normalized exponential function for final layer activation, as opposed to the various sigmoid functions commonly used in binary classification tasks.

Cavanagh et al. (2021) have performed multi-class classification on

[1] `https://www.tensorflow.org/`

[2] `https://keras.io/`

data visually classified by Nair and Abraham (2010) from the SDSS Data Release 4 (Adelman-McCarthy et al. 2006), using a CNN to distinguish between three (elliptical, lenticular and spiral) and four (elliptical, lenticular, spiral and irregular) classes of objects. Four different network architectures are tested, each built using Keras. The tested architectures consist of varying amounts of convolutional and pooling layers, as well as different hyperparameter values. All of the architectures share the same activation function (rectified linear unit) in their convolutional and dense layers, and the same final layer activation function (normalized exponential).

The received results from the four different architectures vary on 3-way classification between 75% and 83% on input image size 100 x 100 and between 81% and 84% with size 200 x 200. With 4-way classification, the results were 74%-81% for 100 x 100 images and 79%-83% for 200 x 200 images. While the classification accuracy for spirals (93% in 3-way, 89% in 4-way) is high, the networks have trouble with lenticular galaxies (60% in both cases) and almost entirely fail to classify irregulars (27% in 4-way) in the 4-way classification. The bad performance on classification of irregulars is, however, more due to a heavily under-representative training set than any shortcomings of the network itself. Cavanagh et al. (2021) remark that the misclassifications can in some cases be interpreted as physically meaningful ones, and that they can be traced to for example effects of redshift or larger than average size of the galaxies. This is seen as a sign that the networks have effectively learned to differentiate galaxies based on the main morphological features of different Hubble types.

4.2.3. Transfer learning

Transfer learning refers to a method where a CNN model is first trained on one problem, after which the model's weights and architecture are applied to a similar problem either by using the old model as is, or by integrating the old model partially or completely into a new model.

The study by Tanoglidis, Ćiprijanović, et al. (2020) presented in chapter 4.2.2 also includes a transfer learning trial. The model trained on DES image data is adapted to classify data from the Hyper-Suprime-Cam survey. The original model is used both with and without retraining it on the HSC image data. Without retraining, the model reaches a classification accuracy of 82,1%, compared to an accuracy of 87.6% after having been retrained on a set of data consisting of 320 objects. The retraining is done with a very small learning rate in order to somewhat maintain the original weights of the model and to avoid overfitting.

Domínguez Sánchez et al. (2019) present another example of transfer

learning applied to cross-survey galaxy classification. The models trained on SDSS data are applied separately to three different classification tasks, each with its own model. Classification is done between galaxies with disks/features and smooth galaxies, between edge-on and face-on galaxies, and lastly between galaxies with bar signature and galaxies with no bar. The SDSS-based models are then applied to DES data, evaluating the performance of the model in four different cases: the original model is directly applied to DES data without retraining, the weights of all the original model's layers are fine-tuned with a small learning rate using a small batch of DES data, only the weights of the fully connected layer are fine-tuned, and the model is fully trained anew with the same small DES sample batch as in the previous two cases.

The models were found to adapt best to new data when all of the model's layers are fine-tuned with a small amount of labeled data from DES. All of the three different classification cases reach an accuracy of 95% with the fine-tuned model, though the precision rate varies between the three. The precision metric indicates what portion of both true and false positive classifications were true positives. Since the classification task is a binary one, false positives and negatives refer to classifications where an objects of for example the smooth class is classified as an object of the disk class, and vice versa.

4.3. Unsupervised learning

Using supervised learning in any automated classification task requires a large amount of pre-classified data for the purpose of training the classification algorithm. This can be circumvented by unsupervised machine learning methods. Unsupervised machine learning refers to a procedure where an algorithm autonomously deduces the key categories from the data presented to it and compresses an arbitrary amount of input data into said categories. Although the effectiveness of any classification algorithm has to eventually be benchmarked by comparing its produced results to pre-classified data or by assessing the quality of the classifications by eye, cutting away the need for one of the two large data batches necessary for supervised learning reduces the amount of time and effort needed to establish an automated classification scheme.

An unsupervised learning scheme can be established in several different ways: these include anomaly detection, clustering, neural network and latent variable methods.

4.3.1. Clustering methods

Clustering methods with significance in astronomy include for example k-means clustering and agglomerative hierarchical clustering. Agglomerative hierarchical clustering (see e.g. Johnson 1967) is a bottom-up algorithm which creates a hierarchical model of clusters. In the case of bottom-up clustering, the algorithm begins each evaluation process from a singular cluster, merging cluster pairs as it climbs up the hierarchy.

Hocking et al. (2018) use a technique combining agglomerative hierarchical clustering (see figure 4.2) with growing neural gas network algorithm (GNG; refer to Fritzke et al. 1995 for a detailed description of the algorithm) and connected component labelling to automatically segment and label galaxies basing only on pixel data. The used technique is first applied to Hubble Space Telescope (HST) Frontier Fields survey images and then further used on HST Cosmic Assembly Near-infrared Deep Extra-galactic Legacy Survey (CANDELS) fields. This technique has later been built upon by for example Martin et al. (2020), who use a similar approach to identify different galaxy types from the Hyper-Suprime-Cam Subaru-Strategic-Program Ultra-Deep layer and sort them into morphological clusters.

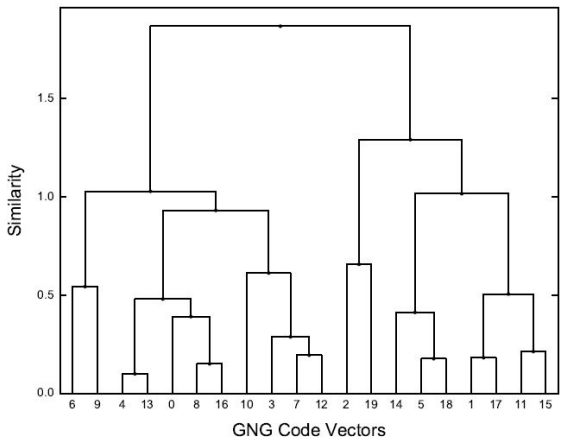

Figure 4.2: Visualization of the hierarchical clustering process by Hocking et al. (2018). The x-axis lists the GNG node identifiers and the y-axis represents the degree of similarity, with the root node at the top.

In the learning phase of the network, the unlabeled training image is converted into a m x n data matrix, where each row of the matrix is a sample vector, serving as a rotation invariant representation of a small patch area of the image, and each column is a feature with a value. The GNG algorithm is then used to create a topological map, which is a k x n

(k < m, k being the number of GNG nodes) data matrix, of the previous matrix. Each sample vector in this matrix represents a cluster of similar small sub-image patches used to create the first matrix. Hierarchical clustering is then on used to further reduce the number of clusters to identify subsets of the groups represented in the data matrix generated by GNG. Connected-component labelling can thus be used to identify the numbers and types of the small sub-image patches which, together, form each galaxy in the survey image.

Another data matrix can be created by creating a sample vector for each galaxy, where each element in a galaxy's sample vector corresponds to one 'type' of a sub-image patch. Several patches form a galaxy, and each sample vector is a histogram of the types of sub-images contained in a galaxy. After normalization of the sample vectors, the result is a matrix where each sample vector is a scale and rotation invariant representation of a galaxy. From this, main groups or types of galaxies can be identified via hierarchical clustering, and the positions of each group used then to identify galaxy types from other, previously unseen images.

Several of the automated groups created by the classifier are found to be in agreement with the consensus classifications of the same data from Galaxy Zoo. Hocking et al. (2018) remark that the algorithm could be of use especially in the search for similar galaxies when the user has a test example in mind, or in the search of undiscovered features.

5. Summary

Galaxies are systems of dark matter, stars, gas and dust orbiting around a central concentration of mass. They span a wide variety of appearances, based on which they can be classified. Several classification schemes have been developed during the last century, with an attempt to relate the different types of galaxies to each other based on their key physical features and use the received information to further the understanding of both the composition as well as the evolution of galaxies. In the past, the small amount of galaxies in survey image data allowed for the classification process to be completed visually, but with the ever-growing size and depth of survey image data, making classifications in this way nowadays is near to impossible.

Various machine learning algorithms specialized in image recognition and classification can outperform human classifiers in terms of speed and likely soon also in accuracy. The advent of the development of neural network tools for astronomy was in early 1990's, and ever since especially convolutional neural networks have been applied to classification problems in galactic astronomy. Applications of unsupervised learning have also shown promise in being able to produce self-organizing classification results. The rapid development of machine learning algorithms and hardware suited to perform automated large-scale classification tasks with astronomical survey data holds promise for machine learning methods being able to eventually fully replace humans in most classification tasks.

References

Abraham, R. G., S. van den Bergh, and P. Nair (May 2003). "A New Approach to Galaxy Morphology. I. Analysis of the Sloan Digital Sky Survey Early Data Release". In: *The Astrophysical Journal* 588.1, pp. 218–229. DOI: 10.1086/373919. arXiv: astro-ph/0301239 [astro-ph].

Adelman-McCarthy, J. K. et al. (Jan. 2006). "The Fourth Data Release of the Sloan Digital Sky Survey". In: *The Astrophysical Journal Supplement Series* 162.1, pp. 38–48. DOI: 10.1086/497917. URL: https://doi.org/10.1086/497917.

Aguerri, J. A. L., M. Balcells, and R. F. Peletier (Feb. 2001). "Growth of galactic bulges by mergers. I. Dense satellites". In: *Astronomy and Astrophysics* 367, pp. 428–442. DOI: 10.1051/0004-6361:20000441. arXiv: astro-ph/0012156 [astro-ph].

Aniyan, A. K. and K. Thorat (June 2017). "Classifying Radio Galaxies with the Convolutional Neural Network". In: *The Astrophysical Journal Supplement Series* 230.2, 20, p. 20. DOI: 10.3847/1538-4365/aa7333. arXiv: 1705.03413 [astro-ph.IM].

Athanassoula, E. (Apr. 2005). "On the nature of bulges in general and of box/peanut bulges in particular: input from N-body simulations". In: *Monthly Notices of the Royal Astronomical Society* 358.4, pp. 1477–1488. DOI: 10.1111/j.1365-2966.2005.08872.x. arXiv: astro-ph/0502316 [astro-ph].

Athanassoula, E., E. Laurikainen, H. Salo, and A. Bosma (Dec. 2015). "On the nature of the barlens component in barred galaxies: what do boxy/peanut bulges look like when viewed face-on?" In: *Monthly Notices of the Royal Astronomical Society* 454.4, pp. 3843–3863. DOI: 10.1093/mnras/stv2231. arXiv: 1405.6726 [astro-ph.GA].

Böker, T. (Aug. 2009). "Nuclear star clusters". In: *Proceedings of the International Astronomical Union* 5.S266, pp. 58–63. ISSN: 1743-9221. DOI: 10.1017/s1743921309990871. URL: http://dx.doi.org/10.1017/S1743921309990871.

Buta, R., S. Mitra, G. de Vaucouleurs, and J. Corwin H. G. (Jan. 1994). "Mean Morphological Types of Bright Galaxies". In: *The Astronomical Journal* 107, p. 118. DOI: 10.1086/116838.

Buta, R. J. (Sept. 2019). "The systematics of galaxy morphology in the comprehensive de Vaucouleurs revised Hubble-Sandage classification system: application to the EFIGI sample". In: *MNRAS* 488.1, pp. 590–608. DOI: 10.1093/mnras/stz1693. arXiv: 1906.08124 [astro-ph.GA].

Buta, R. J., K. Sheth, et al. (Apr. 2015). "A Classical Morphological Analysis of Galaxies in the Spitzer Survey of Stellar Structure in Galaxies (S4G)". In: *APJS* 217.2, 32, p. 32. DOI: 10.1088/0067-0049/217/2/32. arXiv: 1501.00454 [astro-ph.GA].

Cavanagh, M. K., K. Bekki, and B. A. Groves (June 2021). "Morphological classification of galaxies with deep learning: comparing 3-way and 4-way CNNs". In: *arXiv e-prints*, arXiv:2106.01571, arXiv:2106.01571. arXiv: 2106.01571 [astro-ph.GA].

Cheng, T.-Y. et al. (Apr. 2020). "Optimizing automatic morphological classification of galaxies with machine learning and deep learning using Dark Energy Survey imaging". In: *Monthly Notices of the Royal Astronomical Society* 493.3, pp. 4209–4228. DOI: 10.1093/mnras/staa501. arXiv: 1908.03610 [astro-ph.GA].

Comerón, S. et al. (Mar. 2010). "AINUR: Atlas of Images of NUclear Rings". In: *Monthly Notices of the Royal Astronomical Society* 402.4, pp. 2462–2490. DOI: 10.1111/j.1365-2966.2009.16057.x. arXiv: 0908.0272 [astro-ph.CO].

Conselice, C. J. (July 2003). "The Relationship between Stellar Light Distributions of Galaxies and Their Formation Histories". In: *The Astrophysical Journal Supplement Series* 147.1, pp. 1–28. DOI: 10.1086/375001. arXiv: astro-ph/0303065 [astro-ph].

Conselice, C. J., M. A. Bershady, and A. Jangren (Feb. 2000). "The Asymmetry of Galaxies: Physical Morphology for Nearby and High-Redshift Galaxies". In: *The Astrophysical Journal* 529.2, pp. 886–910. DOI: 10.1086/308300. arXiv: astro-ph/9907399 [astro-ph].

Davies, A., S. Serjeant, and J. M. Bromley (Aug. 2019). "Using convolutional neural networks to identify gravitational lenses in astronomical images". In: *Monthly Notices of the Royal Astronomical Society* 487.4, pp. 5263–5271. DOI: 10.1093/mnras/stz1288. arXiv: 1905.04303 [astro-ph.IM].

de Vaucouleurs, G. (Jan. 1959). "Classification and Morphology of External Galaxies." In: *Handbuch der Physik* 53, pp. 275–310. DOI: 10.1007/978-3-642-45932-0_7.

Dieleman, S., K. W. Willett, and J. Dambre (Apr. 2015). "Rotation-invariant convolutional neural networks for galaxy morphology prediction". In: *Monthly Notices of the Royal Astronomical Society* 450.2, pp. 1441–1459. ISSN: 0035-8711. DOI: 10.1093/mnras/stv632. URL: http://dx.doi.org/10.1093/mnras/stv632.

Domínguez Sánchez, H. et al. (Mar. 2019). "Transfer learning for galaxy morphology from one survey to another". In: *Monthly Notices of the Royal Astronomical Society* 484.1, pp. 93–100. DOI: 10.1093/mnras/sty3497. arXiv: 1807.00807 [astro-ph.GA].

Elmegreen, D. M. and B. G. Elmegreen (Dec. 1982). "Flocculent and grand design spiral structure in field, binary and group galaxies." In: *Monthly Notices of the Royal Astronomical Society* 201, pp. 1021–1034. DOI: 10.1093/mnras/201.4.1021.

Elmegreen, D. M., B. G. Elmegreen, and A. Dressler (Dec. 1982). "Flocculent and grand design spiral arm structure in cluster galaxies". In: *Monthly Notices of the Royal Astronomical Society* 201, pp. 1035–1039. DOI: 10.1093/mnras/201.4.1035.

Elmegreen, D. M. and B. G. Elmegreen (Mar. 1987). "Arm Classifications for Spiral Galaxies". In: *Astrophysical Journal* 314, p. 3. DOI: 10.1086/165034.

Elmegreen, D. M., B. G. Elmegreen, D. S. Rubin, and M. A. Schaffer (Sept. 2005). "Galaxy Morphologies in the Hubble Ultra Deep Field: Dominance of Linear Structures at the Detection Limit". In: *The Astrophysical Journal* 631.1, pp. 85–100. DOI: 10.1086/432502. arXiv: astro-ph/0508216 [astro-ph].

Elmegreen, D. M., B. G. Elmegreen, and C. M. Sheets (Mar. 2004). "Chain Galaxies in the Tadpole Advanced Camera for Surveys Field". In: *The Astrophysical Journal* 603.1, pp. 74–81. DOI: 10.1086/381357. arXiv: astro-ph/0401364 [astro-ph].

Erwin, P. et al. (Feb. 2015). "Composite bulges: the coexistence of classical bulges and discy pseudo-bulges in S0 and spiral galaxies". In: *Monthly Notices of the Royal Astronomical Society* 446.4, pp. 4039–4077. DOI: 10.1093/mnras/stu2376. arXiv: 1411.2599 [astro-ph.GA].

Franx, M., G. Illingworth, and T. de Zeeuw (Dec. 1991). "The Ordered Nature of Elliptical Galaxies: Implications for Their Intrinsic Angular Momenta and Shapes". In: *The Astrophysical Journal* 383, p. 112. DOI: 10.1086/170769.

Friedli, D. and L. Martinet (Sept. 1993). "Bars within bars in lenticular and spiral galaxies : a step in secular evolution?" In: *Astronomy and Astrophysics* 277, pp. 27–41.

Fritzke, B. et al. (1995). "A growing neural gas network learns topologies". In: *Advances in neural information processing systems* 7, pp. 625–632.

Graham, A. W. (Aug. 2019). "A galaxy classification grid that better recognizes early-type galaxy morphology". In: *Monthly Notices of the Royal Astronomical Society* 487.4, pp. 4995–5009. DOI: 10.1093/mnras/stz1623. arXiv: 1907.09791 [astro-ph.GA].

Grebel, E. K., J. S. Gallagher III, and D. Harbeck (Apr. 2003). "The Progenitors of Dwarf Spheroidal Galaxies". In: *The Astronomical Journal* 125.4, pp. 1926–1939. DOI: 10.1086/368363. arXiv: astro-ph/0301025 [astro-ph].

Hocking, A., J. E. Geach, Y. Sun, and N. Davey (Jan. 2018). "An automatic taxonomy of galaxy morphology using unsupervised machine learning". In: *Monthly Notices of the Royal Astronomical Society* 473.1, pp. 1108–1129. DOI: 10.1093/mnras/stx2351. arXiv: 1709.05834 [astro-ph.IM].

Hubble, E. P. (Dec. 1926). "Extragalactic nebulae." In: *Astrophysical Journal* 64, pp. 321–369. DOI: 10.1086/143018.

— (1936). *Realm of the Nebulae*. Yale University Press.

Impey, C. and G. Bothun (Jan. 1997). "Low Surface Brightness Galaxies". In: *Annual Review of Astronomy and Astrophysics* 35, pp. 267–307. DOI: 10.1146/annurev.astro.35.1.267.

Johnson, S. C. (1967). "Hierarchical clustering schemes". In: *Psychometrika* 32.3, pp. 241–254.

Kormendy, J. and R. Bender (June 1996). "A Proposed Revision of the Hubble Sequence for Elliptical Galaxies". In: *Astrophysical Journal* 464, p. L119. DOI: 10.1086/310095.

— (Jan. 2012). "A Revised Parallel-sequence Morphological Classification of Galaxies: Structure and Formation of S0 and Spheroidal Galaxies". In: *The Astrophysical Journal Supplement* 198.1, 2, p. 2. DOI: 10.1088/0067-0049/198/1/2. arXiv: 1110.4384 [astro-ph.CO].

Kurtz, M. J. (Nov. 1983). "Classification methods: An introductory survey (Review)". In: *Statistical Methods in Astronomy*. Ed. by E. J. Rolfe, p. 47.

Lahav, O. et al. (Feb. 1995). "Galaxies, Human Eyes, and Artificial Neural Networks". In: *Science* 267.5199, pp. 859–862. DOI: 10.1126/science.267.5199.859. arXiv: astro-ph/9412027 [astro-ph].

Laurikainen, E., H. Salo, R. Buta, and J. H. Knapen (Dec. 2011). "Near-infrared atlas of S0-Sa galaxies (NIRS0S)". In: *Monthly Notices of the Royal Astronomical Society* 418.3, pp. 1452–1490. ISSN: 0035-8711. DOI: 10.1111/j.1365-2966.2011.19283.x.

Lin, C. C., C. Yuan, and F. H. Shu (Mar. 1969). "On the Spiral Structure of Disk Galaxies. III. Comparison with Observations". In: *Astrophysical Journal* 155, p. 721. DOI: 10.1086/149907.

Lisker, T. (Dec. 2008). "Is the Gini Coefficient a Stable Measure of Galaxy Structure?" In: *The Astrophysical Journal Supplement Series* 179.2, pp. 319–325. DOI: 10.1086/591795. arXiv: 0807.1531 [astro-ph].

Loebman, S. R., R. Roškar, V. P. Debattista, Ž. Ivezić, T. R. Quinn, and J. Wadsley (Aug. 2011). "The Genesis of the Milky Way's Thick Disk Via Stellar Migration". In: *The Astrophysical Journal* 737.1, 8, p. 8. DOI: 10.1088/0004-637X/737/1/8. arXiv: 1009.5997 [astro-ph.GA].

Lotz, J. M., J. Primack, and P. Madau (July 2004). "A New Nonparametric Approach to Galaxy Morphological Classification". In: *The Astronomical Journal* 128.1, pp. 163–182. DOI: 10.1086/421849. arXiv: astro-ph/0311352 [astro-ph].

Mac Low, M.-M. and R. McCray (Jan. 1988). "Superbubbles in Disk Galaxies". In: *Astrophysical Journal* 324, p. 776. DOI: 10.1086/165936.

Martin, G., S. Kaviraj, A. Hocking, S. C. Read, and J. E. Geach (Jan. 2020). "Galaxy morphological classification in deep-wide surveys via unsupervised machine learning". In: *Monthly Notices of the Royal Astronomical Society* 491.1, pp. 1408–1426. DOI: 10.1093/mnras/stz3006. arXiv: 1909.10537 [astro-ph.GA].

McCarthy, I. G., A. S. Font, R. A. Crain, A. J. Deason, J. Schaye, and T. Theuns (Mar. 2012). "Global structure and kinematics of stellar haloes in cosmological hydrodynamic simulations". In: *Monthly Notices of the Royal Astronomical Society* 420.3, pp. 2245–2262. DOI: 10.1111/j.1365-2966.2011.20189.x. arXiv: 1111.1747 [astro-ph.GA].

Morgan, W. W. (Aug. 1958). "A Preliminary Classification of the Forms of Galaxies According to Their Stellar Population". In: *Publications of the Astronomical Society of the Pacific* 70.415, p. 364. DOI: 10.1086/127243.

— (Dec. 1971). "A Unitary Classification for N Galaxies". In: *Astronomical Journal* 76, p. 1000. DOI: 10.1086/111214.

Müller, O. and E. Schnider (Feb. 2021). "Dwarfs from the Dark (Energy Survey): a machine learning approach to classify dwarf galaxies from multi-band image". In: *arXiv e-prints*, arXiv:2102.12776, arXiv:2102.12776. arXiv: 2102.12776 [astro-ph.GA].

Naim, A., O. Lahav, J. Sodre L., and M. C. Storrie-Lombardi (Aug. 1995). "Automated morphological classification of APM galaxies by supervised artificial neural networks". In: *Monthly Notices of the Royal Astronomical Society* 275.3, pp. 567–590. DOI: 10.1093/mnras/275.3.567. arXiv: astro-ph/9503001 [astro-ph].

Nair, P. B. and R. G. Abraham (Feb. 2010). "A Catalog of Detailed Visual Morphological Classifications for 14,034 Galaxies in the Sloan

Digital Sky Survey". In: *The Astrophysical Journal Supplement* 186.2, pp. 427–456. DOI: 10.1088/0067-0049/186/2/427. arXiv: 1001.2401 [astro-ph.CO].

Noguchi, M. (Mar. 1999). "Early Evolution of Disk Galaxies: Formation of Bulges in Clumpy Young Galactic Disks". In: *The Astrophysical Journal* 514.1, pp. 77–95. DOI: 10.1086/306932. arXiv: astro-ph/9806355 [astro-ph].

Odewahn, S. C., E. B. Stockwell, R. L. Pennington, R. M. Humphreys, and W. A. Zumach (Jan. 1992). "Automated Star/Galaxy Discrimination With Neural Networks". In: *The Astronomical Journal* 103, p. 318. DOI: 10.1086/116063.

Peletier, R. et al. (Aug. 2020). "The Fornax Deep Survey data release 1". In: *arXiv e-prints*, arXiv:2008.12633, arXiv:2008.12633. arXiv: 2008.12633 [astro-ph.GA].

Petrillo, C. E. et al. (Oct. 2018). "Testing Convolutional Neural Networks for finding strong gravitational lenses in KiDS". In: *Monthly Notices of the Royal Astronomical Society*. ISSN: 1365-2966. DOI: 10.1093/mnras/sty2683. URL: http://dx.doi.org/10.1093/mnras/sty2683.

Putman, M. E., J. E. G. Peek, and M. R. Joung (Sept. 2012). "Gaseous Galaxy Halos". In: *Annual Review of Astronomy and Astrophysics* 50, pp. 491–529. DOI: 10.1146/annurev-astro-081811-125612. arXiv: 1207.4837 [astro-ph.GA].

Reynolds, J. H. (June 1925). "The forms and development of the spiral and allied nebulae". In: *Monthly Notices of the Royal Astronomical Society* 85, pp. 1014–1020. DOI: 10.1093/mnras/85.12.1014.

Sandage, A. and B. Binggeli (July 1984). "Studies of the Virgo cluster. III. A classification system and an illustrated Atlas of Virgo cluster dwarf galaxies." In: *The Astronomical Journal* 89, pp. 919–931. DOI: 10.1086/113588.

Sandage, A., K. C. Freeman, and N. R. Stokes (June 1970). "The Intrinsic Flattening of e, so, and Spiral Galaxies as Related to Galaxy Formation and Evolution". In: *Astrophysical Journal* 160, p. 831. DOI: 10.1086/150475.

Schweizer, F., J. Ford W. Kent, R. Jedrzejewski, and R. Giovanelli (Sept. 1987). "The Structure and Evolution of Hoag's Object". In: *The Astrophysical Journal* 320, p. 454. DOI: 10.1086/165562.

Seigar, M. S. and P. A. James (Sept. 1998). "The structure of spiral galaxies - II. Near-infrared properties of spiral arms". In: *Monthly Notices of the Royal Astronomical Society* 299.3, pp. 685–698. DOI: 10.1046/j.1365-8711.1998.01779.x. arXiv: astro-ph/9803254 [astro-ph].

Seigar, M. S., D. Kennefick, J. Kennefick, and C. H. S. Lacy (May 2008). "Discovery of a Relationship between Spiral Arm Morphology and Supermassive Black Hole Mass in Disk Galaxies". In: *The Astrophysical Journal Letters* 678.2, p. L93. DOI: 10.1086/588727. arXiv: 0804.0773 [astro-ph].

Shapiro, P. R. and G. B. Field (May 1976). "Consequences of a New Hot Component of the Interstellar Medium". In: *Astrophysical Journal* 205, pp. 762–765. DOI: 10.1086/154332.

Shapley, H. (Oct. 1938). "Two Stellar Systems of a New Kind". In: *Nature* 142.3598, pp. 715–716. DOI: 10.1038/142715b0.

Tanoglidis, D., A. Drlica-Wagner, et al. (Jan. 2021). "Shadows in the Dark: Low-surface-brightness Galaxies Discovered in the Dark Energy Survey". In: *The Astrophysical Journal Supplement Series* 252.2, p. 18. ISSN: 1538-4365. DOI: 10.3847/1538-4365/abca89. URL: http://dx.doi.org/10.3847/1538-4365/abca89.

Tanoglidis, D., A. Ćiprijanović, and A. Drlica-Wagner (2020). *DeepShadows: Separating Low Surface Brightness Galaxies from Artifacts using Deep Learning*. arXiv: 2011.12437 [astro-ph.GA].

Tremaine, S. D., J. P. Ostriker, and J. Spitzer L. (Mar. 1975). "The formation of the nuclei of galaxies. I. M31." In: *Astrophysical Journal* 196, pp. 407–411. DOI: 10.1086/153422.

van den Bergh, S. (June 1976). "A new classification system for galaxies." In: *Astrophysical Journal* 206, pp. 883–887. DOI: 10.1086/154452.

— (1998). *Galaxy Morphology and Classification*. Cambridge University Press. ISBN: 9780521623353.

— (Aug. 2002). "Ten Billion Years of Galaxy Evolution". In: *The Publications of the Astronomical Society of the Pacific* 114.798, pp. 797–802. DOI: 10.1086/341708. arXiv: astro-ph/0204315 [astro-ph].

Villalobos, Á. and A. Helmi (Mar. 2008). "Simulations of minor mergers. I. General properties of thick disks". In: *arXiv e-prints*, arXiv:0803.2323, arXiv:0803.2323. arXiv: 0803.2323 [astro-ph].

Walmsley, M. et al. (Oct. 2019). "Galaxy Zoo: probabilistic morphology through Bayesian CNNs and active learning". In: *Monthly Notices of the Royal Astronomical Society* 491.2, pp. 1554–1574. ISSN: 1365-2966. DOI: 10.1093/mnras/stz2816. URL: http://dx.doi.org/10.1093/mnras/stz2816.

Weir, N., U. M. Fayyad, and S. Djorgovski (June 1995). "Automated Star/Galaxy Classification for Digitized Poss-II". In: *Astronomical Journal* 109, p. 2401. DOI: 10.1086/117459.

Yoachim, P. and J. J. Dalcanton (Jan. 2006). "Structural Parameters of Thin and Thick Disks in Edge-on Disk Galaxies". In: *The Astro-*

nomical Journal 131.1, pp. 226–249. DOI: 10.1086/497970. arXiv: astro-ph/0508460 [astro-ph].